CORNELL'S BEAM LINE HIGHER ORDER MODE ABSORBERS

G.R. Eichhorn#, J. Conway, Y. He, Y. Li, T. O'Connell, P. Quigley,
J. Sears, V.D. Shemelin, N.R.A. Valles
Cornell Laboratory for Accelerator-Based Sciences and Education, Cornell University
Ithaca, NY 14853-5001, USA

Abstract

Efficient damping of the higher-order modes (HOMs) of the superconducting cavities is essential for the proposed energy recovery linac at Cornell that aims for high beam currents and short bunches. Designing these HOM beamline absorbers has been a long endeavor, sometimes including disappointing results. We will review the design, the findings on the prototype and the final choices made for the 7 HOM absorbers being built for the main linac cryomodule (MLC) prototype.

INTRODUCTION

The potential for excellent quality of X-ray beams, generated by a low-emittance electron beam, motivated the design of a 5-GeV superconducting energy-recovery linac (ERL) [1] at Cornell University. Starting with 15 MeV electrons produced by a photo-injector with currents of up to 100 mA [2], the beam will be accelerated in two main linac sections to 5 GeV before it enters several undulators feeding the X-ray beamlines. The existing CESR ring is then used to return the beam and inject it into additional undulators, before it gets decelerated to 15 MeV again inside the two main linac sections. A more detailed description can be found in the recently updated project definition design report [3]. Due to the high beam current combined with the short bunch operation, a careful control and efficient damping of the higher-order modes (HOMs) is essential. This paper focuses on the properties of these dampers.

In high current storage rings with superconducting cavities (like CESR @ Cornell) strong broadband HOM damping has been achieved by using beam-pipe ferrite loads operating at room temperature [4]. The ERL will adopt the same damping concept with RF absorbers between the cavities in a cavity string. This will require operating the absorbers at a temperature of about 80 K which has been proven in the injector cryomodule (ICM) [5]. We updated the absorber design for the main linac cryomodule (MLC) [6].

LESSEONS FROM THE PROTOTYPE

For the Horizontal Test Cryomodule (HTC) [7], three of these absorbers- as show in Fig. 1 were prototyped. Two of there were mounted into the module and have so far proven to be an efficient RF damper. In the HTC-3 experiment, we measured the higher order mode spectrum of our 7-cell cavity and compared it to a measured spectrum without dampers. Up to 3.7 GHz we found no dipole resonances with Qs above 10^4 indicating the absorber provides suitable RF damping [8]. However, the design issues became visible: during the mounting process we broke one absorber by over-torqueing the flange connection as the assembly was leaking. After a careful investigation we found the reason for this leakage: to closely match the thermal expansion coefficient of the absorber material (silicon carbide, SiC), we prazed it to tungsten which also acts as a vacuum barrier and holds the knife edge of the flange transition to the stainless, Originally being tight we discovered that this sintered tungsten material becomes porous under the thermal cycle of the brazing (which is done at 750 C).

For the HTC, the two absorbers were sprayed extensively with vacuum sealant to bring the leak-rate down to an acceptable number- leading however to a beam vacuum to insulation vacuum leakage which complicates future mounting processes.

In addition to these mechanical and vacuum issues we found that the silicon carbide we used (SC-35 from Coorstek) showed a marginally high dc resistivity at 77 K- which remarkably differs from what we measured on small samples. This bears the risk of charging up the material once an electron beam passes through the absorber. This batch to batch variation was also reported by colleagues and seems to be intrinsic to the fabrication procedure.

The redesign efforts therefore concentrated on two: investigating alternative absorber materials and changing the transition to the vacuum barrier.

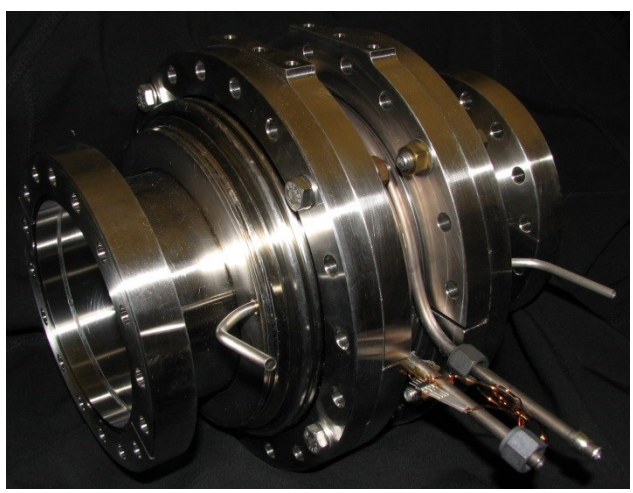

Figure 1: Cross-section of the HOM absorber currently being installed in the Horizontal Test Cryomodule (HTC). The absorbing material is SiC brazed to tungsten.

#r.eichhorn@cornell.edu

ISBN 978-3-95450-143-4

RF ABSORBING MATERIAL

The search for a suitable RF absorbing material has been a long endeavour. Initial results have been published earlier [7, 8]. Based on out application, the material should have a broad band of absorption (with frequencies up to 50 GHz) but on the other hand a good DC conductivity to ensure that no charges are collected even if some particles of the beam hit the surface

So far, the most promising material seems to be a graphite loaded SiC ceramic (Coorstek® SC-35). However, the dc conductivity we measured on a sample ordered a year ago (being some kΩ at 77 K) was not reproducible. We therefore tested the similar material SC-2 which was advertised as low resistivity material. This was confirmed, however, the rf absorption properties described below disqualified the material.

Table 1 summarizes our findings on the dc conductivity measurements, including the AlN based material Ceradyne® CS-137 that will be used in the X-FEL linac.

Table 1: Measured dc Conductivity of the Different Materials (along the 130 mm length)

Material	300 K	77 K
Coorstek SiC SC-2	49 Ω	59 Ω
Coorstek SiC SC-35	~100 kΩ	Infinite
Ceradyne AlN CS-137	5.7 kΩ	7 kΩ

RESONANCE MEASUREMENTS OF A COMPLEX EPSILON

During the qualifying phase of the different material we developed a highly accurate set-up to measure the complex epsilon using transmission lines [9, 10].

However, as the material received so far varied significantly in its properties we developed a method to measure the absorption without cutting it into samples. The basic idea behind this method is to analyse the change in the eigenfrequencies and the quality factors of a pillbox resonate as the material is introduced.

We used the CLANS code, a code from the SLANS family [11] for calculation of the eigenfrequencies f and Q-factors of a cavity consisting of a pillbox with a ceramic cylinder inside. Values of f and Q were found with CLANS for different values of the real (ε`) and imaginary (ε``) parts of the dielectric permittivity of the material and plotted on the graph shown in Figure 2.

By comparing the measured f and Q of a mode with the calculated matrix, the corresponding permittivity was deducted. Figure 2 also includes the measured point for the AlN cylinder: The resonance at 1482 MHz showed an ε = 39 − 7i.

To confirm the validity of the new measurement technique, the AlN cylinder was cut into small samples and conventional transmission line measurements were taken, the results of which are given in Fig. 3. The agreement to the resonant method is quite good. It should be noted that the discontinuities observed at rf band transitions reported earlier could be reduced significantly by correcting for air-gaps and size-inaccuracies. As part of this, all samples now are measured with a CMM machine.

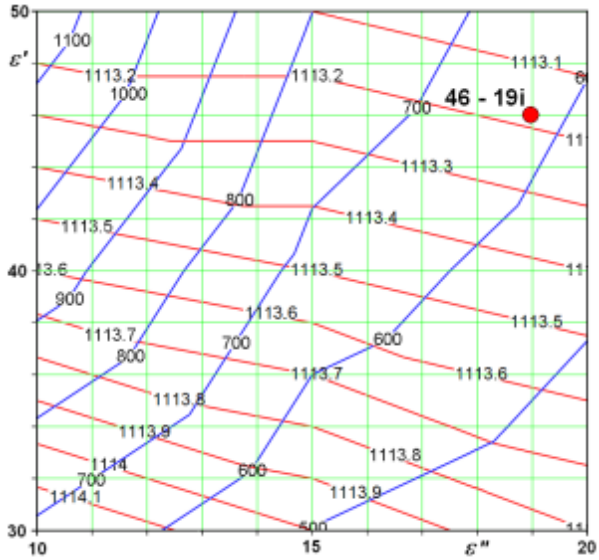

Figure 2: Calculated eigenfrequencies (red) and quality factors (blue) of the pillbox eigenfrequencies with a ceramic cylinder inserted as a function of the real and imaginary part of the dielectric permittivity.

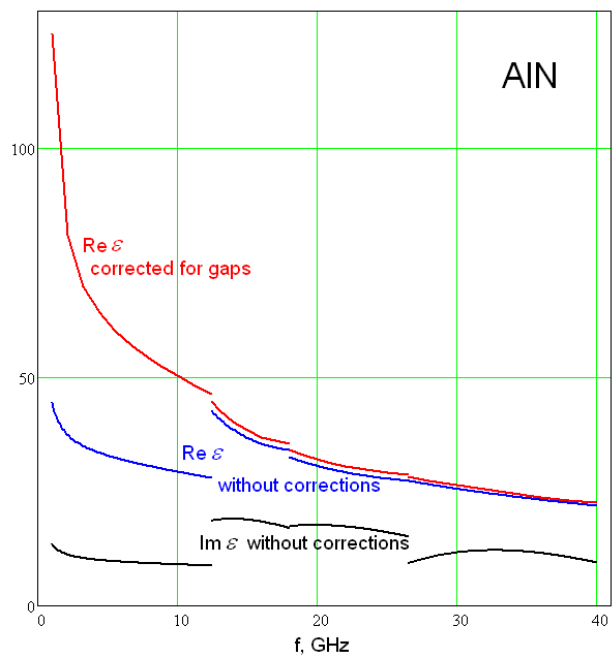

Figure 3: Measured dielectric permittivity as a function of the frequency using the transmission line method. Corrections were made concerning sample size variations which caused discontinuities at rf band transitions if not compensated.

Using the resonant method the SC-2 material mentioned above was measured, leading to a plot shown in Fig. 4- which also shows the limitation of the method. For extremely high imaginary (ε``) parts of the dielectric

permittivity the f and Q curves become parallel, preventing the extraction of this parameter from the measurement.

However, out of this finding one can conclude that the SC-2 silicon carbide is far too conductive and acts more like a bad metal than as a good rf absorber. In practice this would mean that most of the incoming rf is not absorbed but reflected.

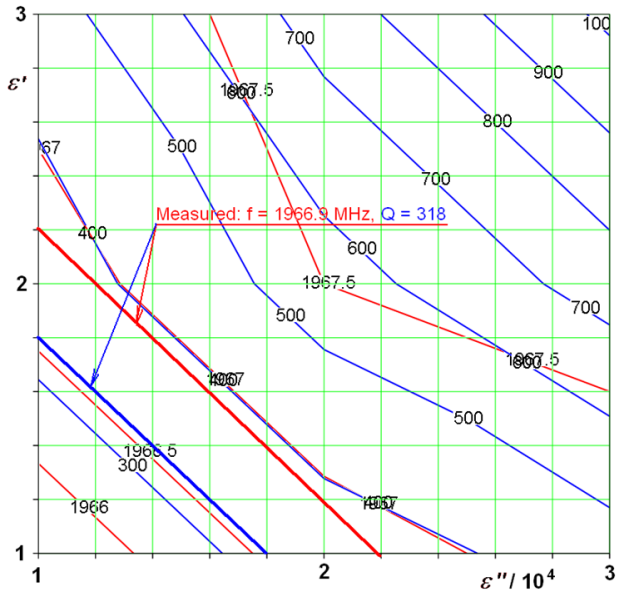

Figure 4: Calculated eigenfrequencies (red) and quality factors (blue) of the pillbox eigenfrequencies in the high imaginary dielectric permittivity regime, compared to the measured parameter of the SC-2 material.

HOM DESIGN FOR THE MAIN LINAC CRYOMODULE

As a consequence of the data presented above, the only material fulfilling the requirements is the AlN. The production HOM (Fig. 5) design has a titanium cooling

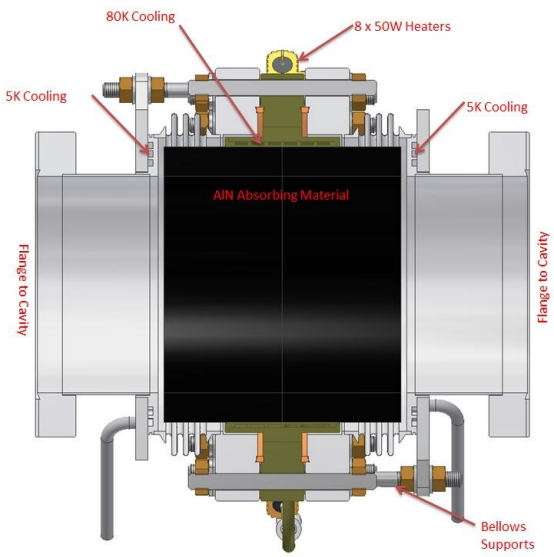

Figure 5: Cross section of the Production beam line HOM absorber design.

Table 2: Working Spread-sheet for the Shrink-fit Parameters, Giving the Formula and the Parameters Used.

Inputs	300K	80K	
SiC inner radius, r_i	2.165	2.165	in
SiC outer radius, Nominal radius R	2.362	2.362	in
Ti tube inner radius, R_{Ti}	2.360	2.356	in
Ti tube outer radius, r_o	2.610	2.606	in
Axial length of contact surface, L	2.421	2.421	in
Coefficient of friction between the two parts, f>	0.1	0.1	
Torsional coefficient of friction between the two parts, f'>	0.1	0.1	
Constants			
Modulus of elasticity, E_{Ti}, Ti Grade 5 Ti-6Al-4V	114	136.8	GPa
Coefficient of linear thermal expansion, α_{SiC}, ceramic SiC	3.8		x10^{-6}/C
Coefficient of linear thermal expansion, α_{Ti}	7.47	4.184	x10^{-6}/C
Outputs			
Radial interference, δ	0.002	0.005	in
Heating temperature for zero clearance, if heat only Ti tube, $\Delta T = \frac{\delta}{R*\alpha_{Ti}}$	138		deg C
Heating temperature for zero clearnace, if heat both tubes, $\Delta T = \frac{\delta}{R*(\alpha_{Ti}-\alpha_{SiC})}$	256		
Radial pressure on interfering surface, $P = \frac{E*\delta}{R}\left[\frac{(r_o^2-R^2)*(R^2-r_i^2)}{2R^2*(r_o^2-r_i^2)}\right]$	4	14	MPa
Maximum compressive stress on SiC, $\sigma_{SiC} = \frac{2PR^2}{(R^2-r_i^2)}$	56	181	MPa
Maximum tensile stress on Ti tube, $\sigma_{Ti} = \frac{P(r_o^2+R^2)}{(r_o^2-R^2)}$	45	147	MPa
Axial holding power, $F=2\pi LRP f$>	10373	33514	N
Torsional holding power, $2\pi LR^2P f'$>	622	2010	N-m

jacket and flange that is thermally shrink fit to the AlN absorber. This central flange gives room for 3 convolution bellows on either side, adding flexibility that was needed in the prototype. The central flange is also the mounting place for 8 - 50W heaters and the vertical support that will mount it to the above helium gas return pipe.

The thermal fit has been designed so that all pieces hold together during a bake up to 150°C and all parts have at least a factor of safety of 2 to yield when cooled to 80K. A radial interference of 0.002in between the titanium cooling jacket and AlN absorber meets these parameters. Our calculations are summarized in tab. 2, Fig. 6 shows a picture of the latest shrink fit assembly as it came out of the oven.

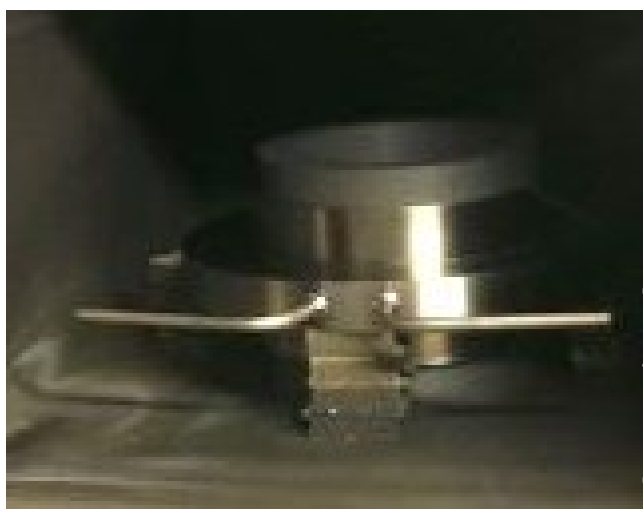

Figure 6: Shrink fit assembly of the SiC into a Ti-5 cylinder, consisting of two shelves welded together with cooling channels in-between and pipes connected to it.

ISBN 978-3-95450-143-4

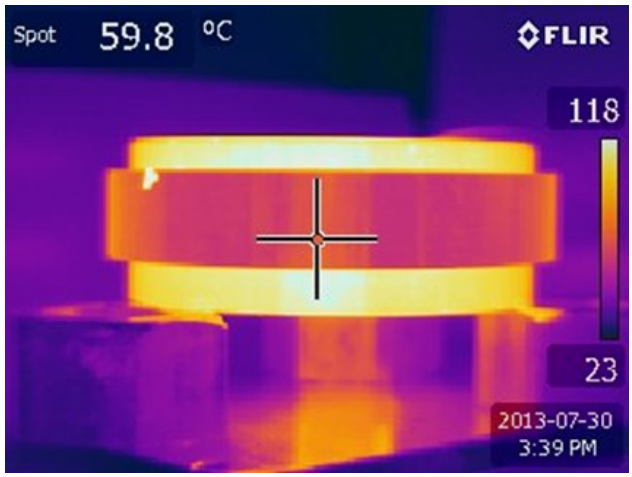

Figure 7: Test of the thermal contact between the absorber and the TI shelve indicating that the shrink fit lead to a uniform mechanical contact with good thermal conduction properties.

To test the features, we have built a prototype Ti-SiC shrink fit assembly and done several thermal cycles from room temp to 77K without seeing any signs of deformation or damage. We used the SiC instead of the AlN as the later was not yet available in the final geometry. This approach is justified as the mechanical parameters of both materials are almost equal.

To check the isotropy of the thermal contact a series of heaters were glued to the inner surface of the absorber. Fig. 7 shows the infrared thermometry picture we took, indicating an uniform heat transfer between the ceramics and the titanium shelve which will have internal cooling channels and cooled by 80 K, 3 bar helium.

Finally, we have done vacuum tests of the prototype and see no signs of trapped gas in the shrink fit joint. In our vacuum test we found the SiC to be hygroscopic and that with a bakeout the outgassing rate can be reduced significantly (Fig. 8). In addition, no vacuum bursting could be observed, indicating that there are no trapped gasses at the shrink fit interface.

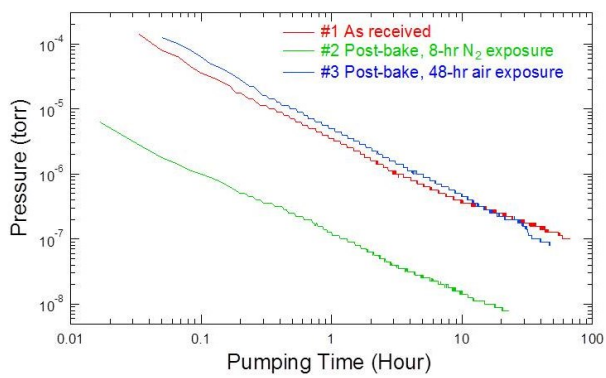

Figure 8: Pumpdown and outgassing test of the shrink-fit assembly. Besides the porous behaviour of the SiC no signs of gas burbs from the shrink-fit could be observed.

SUMMARY

The design of the higher order mode beamline absorbers for the Cornell ERL main linac module has been revised slightly: The absorbing material will now be AlN instead of SiC shrink-fitted into a Ti-5 cylinder. So far the design has been tested successful. Currently, 8 HOM absorber assemblies are under fabrication.

ACKNOWLEDGEMENT

The program is funded by the NSF under grant DMR-0807731. In addition, the authors would like to thank Jacek Sekutowicz for many fruitful discussions.

REFERENCES

[1] Tigner, M. “A Possible Apparatus for Electron Clashing-Beam Experiments”, Nuovo Cimento, 37 -3 (1965) 1221.
[2] B. Dunham et al., “Record high-average current from a high-brightness photoinjector,” App. Phys. Lett. 102 034105 (2013).
[3] G. H. Hoffstaetter, S. Gruner, M. Tigner, eds., Cornell ERL Project Definition Design Report (2013) http://erl.chess.cornell.edu/PDDR/PDDR.pdf
[4] D. Moffat et al. ,” Design and Fabrication of a Ferrite-Lined HOM Load for CESR-B” Proc. of the PAC 993 (1993) 977.
[5] H. Padamsee et al.,” Status of the Cornell ERL Injector Cryomodule” Proc. of the SRF 2007 (2007) 9.
[6] R. Eichhorn et. al, “The CW Linac Cryo-module for Cornell’s ERL”, Proc. of the IPAC 2013 (2013).
[7] N. Valles, et. al. “Record Quality Factor Performance of the Prototype Cornell ERL Main Linac Cavity in the Horizontal Test Cryomodule”, Proc of the SRF 2013 Conf. (2013), submitted.
[8] N. Valles et. al., "HOM Studies of the Cornell ERL Main Linac Cavity: HTC-1 through HTC-3”, Proc. of the IPAC 2013 (2013).
[9] V. Shemelin et. al. “Measurement of ε and μ of lossy Materials for the Cryogenic HOM Load”, Proc. Of the PAC 2005 (2005) 3462.
[10] V. Shemelin, et. al., “Characterization of Ferrites at Low Temperature and High Frequency”, NIM A 557 268-271 (2006).
[11] www.euclidtechlabs.com/SLANS/slans.php.